



PERGAMON

Deep-Sea Research II 49 (2002) 81–105

DEEP-SEA RESEARCH
PART II

www.elsevier.com/locate/dsr2

Tracking the SeaWiFS record with a coupled physical/biogeochemical/radiative model of the global oceans

Watson W. Gregg

NASA/Goddard Space Flight Center, Laboratory for Hydrospheric Processes, Greenbelt, MD 20771, USA

Accepted 16 June 2001

Abstract

The Sea-Viewing Wide Field-of-view Sensor (SeaWiFS) has observed multiple years of routine global chlorophyll observations from space. The mission was launched into a record El Niño event, which eventually gave way to one of the most intense and longest-lasting La Niña events ever recorded. The SeaWiFS chlorophyll record captured the response of ocean phytoplankton to these significant events in the tropical Indo-Pacific basins, but also indicated significant interannual variability unrelated to the El Niño/La Niña events. This included large variability in the North Atlantic and Pacific basins, in the North Central and equatorial Atlantic, and milder patterns in the North Central Pacific.

This SeaWiFS record was tracked with a coupled physical/biogeochemical/radiative model of the global oceans using near-real-time forcing data such as wind stresses, sea surface temperatures, and sea ice. This provided an opportunity to offer physically and biogeochemically meaningful explanations of the variability observed in the SeaWiFS data set, since the causal mechanisms and interrelationships of the model are completely understood.

The coupled model was able to represent the seasonal distributions of chlorophyll during the SeaWiFS era, and was capable of differentiating among the widely different processes and dynamics occurring in the global oceans. The model was also reasonably successful in representing the interannual signal, especially when it was large, such as the El Niño and La Niña events in the tropical Pacific and Indian Oceans. The model provided different phytoplankton group responses for the different events in these regions: diatoms were predominant in the tropical Pacific during the La Niña, but other groups were predominant during El Niño. The opposite condition occurred in the tropical Indian Ocean. Both situations were due to the different responses of the basins to El Niño. Interannual variability in the North Pacific was exhibited as an increase in the spring bloom in 1999 and 2000 relative to 1998. This resulted in the model from a shallower and more rapidly shoaling mixed layer, producing more average irradiance in the water column and preventing herbivore populations to keep pace with increasing phytoplankton populations. However,

E-mail address: gregg@cabin.gsfc.nasa.gov (W.W. Gregg).

several aspects of the interannual cycle were not well-represented by the model. Explanations range from inherent model deficiencies, to monthly averaging of forcing fields, to biases in SeaWiFS atmospheric correction procedures. © 2001 Published by Elsevier Science Ltd.

1. Introduction

The Sea-Viewing Wide Field-of-view Sensor (SeaWiFS; McClain et al., 1998) has provided the first multi-year global chlorophyll observations from space since the Coastal Zone Color Scanner (CZCS). It represents an unprecedented data set in terms of coverage, continuity, and duration that enables us for the first time to make meaningful observations about the state of biological components in the global oceans, their spatial variability, and their medium-term (seasonal to interannual) variability. This latter point especially differentiates SeaWiFS from the two previous large-scale-coverage missions, the CZCS, which did not provide routine global coverage in its 8-year lifetime (Feldman et al., 1989), and the Ocean Color and Temperature Scanner (OCTS), which failed after nine months of on-orbit operations (Shimoda, 1999).

The comprehensive SeaWiFS data set, beginning in September 1997, provides an opportunity to observe the behavior of ocean phytoplankton in response to seasonal and interannual variability. If analysis of this record is combined with the outputs of a coupled physical/biogeochemical model whose dynamical features are completely understood, then insights may be gained into the causes of this variability, especially when the results are in agreement. Even when they are not, this combination of analysis methodologies can help us infer what processes are not incorporated into the model and their apparent importance.

Such application of coupled three-dimensional physical/biological models on basin (e.g., Dutkiewicz et al., 2001; McGillicuddy et al., 1995; Sarmiento et al., 1993) and regional scales (e.g., Walsh et al., 1999; Gregg and Walsh, 1992) has achieved considerable success relating outputs to in situ and satellite observations. In this paper we adapt an existing coupled physical/biogeochemical/radiative model of the global oceans (Gregg, 2000) to the atmospheric and oceanic forcing conditions present during the SeaWiFS era from September 1997 to June 2000 and track the results as compared to SeaWiFS chlorophyll data on synoptic and basin scales. The fact that SeaWiFS in its short lifetime has experienced significant anomalous conditions (El Niño and La Niña) provides an enhanced opportunity to evaluate the nature of the dynamical processes involved and the interactions of biological processes with physical ones.

2. Materials and methods

2.1. SeaWiFS data

SeaWiFS monthly mean chlorophyll data were obtained from the NASA/Goddard Space Flight Center (GSFC)/Distributed Active Archive Center (DAAC). The data set was Version 3, which included several improvements in atmospheric correction and bio-optical algorithms (McClain et al., 2000a,b; O'Reilly et al., 2000), and was completed in May 2000. Level-3 monthly mean SeaWiFS chlorophyll data were re-gridded from the native 4096×2048 grid (approximately 10 km) onto the model grid (see below).

2.2. Coupled physical/biogeochemical model

The coupled global physical/biogeochemical/radiative model is based on Gregg (2000). Although a complete description is contained above, a brief overview is included here for convenience.

The Ocean General Circulation Model (OGCM) is a reduced gravity representation of circulation fields, and is nearly global in scale, extending from near the South Pole to 72°N, in increments of 2/3° latitude and 1 1/4° longitude (Schopf and Lough, 1995). Only ocean areas with depths exceeding 200 m are active. The model contains 14 vertical layers, in quasi-isopycnal coordinates, with the deepest interface in the model at a mean depth of 2800 m. The surface layer represents the upper mixed layer, then there are several layers of fixed thickness to prevent outcropping, and the remaining layer depths are based on the density distribution. The water beneath the deepest interface is assumed to sustain no pressure gradients (i.e. a reduced gravity approximation). Vertical mixing is Richardson number-dependent, following Pacanowski and Philander (1981), and is performed in a time splitting mode, occurring every 12 h in contrast to the 0.5 h Δt of the advective processes. The surface layer temperature of the model relaxes to sea surface temperature.

The biogeochemical model utilizes the circulation fields and the vertical mixing processes to produce horizontal and vertical distributions of constituents. The biogeochemical constituents have their own local dynamical processes. There are 3 phytoplankton groups, diatoms, chlorophytes, and cyanobacteria, which differ in maximum growth rates, sinking rates, and optical properties to help us represent the extreme variety of physical environments encountered in a global model. Cyanobacteria in this model are considered to be very small prokaryotic picoplankton including prochlorophytes. Chlorophytes are assumed to be a diverse group including flagellates. Three nutrients are included to simulate “new” use of nitrogen (Dugdale and Goering, 1967; Eppley and Peterson, 1979) represented by nitrate, regenerated nitrogen represented by ammonium, and silicate as an additional requirement of diatoms. Phytoplankton are ingested by a separate herbivore component, which also contributes to the ammonium field through excretion. Death by senescence contributes a small portion to the ammonium pool, but mostly to the detrital pool, which is ultimately remineralized back to original nutrients. The biogeochemical model has 8 state variables in the fully coupled model.

The model has 3 photoadaptation classes: 50, 150 and 200 ($\mu\text{mol quanta m}^{-2} \text{s}^{-1}$). We compute the mean irradiance during daylight hours, and then classify the phytoplankton photoadaptive state accordingly. This calculation is only performed once per day to simulate a delayed photoadaptation response. Correspondingly, carbon:chlorophyll ratios are related directly to the photoadaptation state. This simulates the behavior of phytoplankton to preferentially synthesize chlorophyll in low light conditions, to enable more efficient photon capture. These three C:chl states are 25, 50 and 80. The C:chl classification is important for evaluating primary production, but more immediately, determining the nutrient:chlorophyll ratios, which are computed assuming the Redfield elemental balances.

Growth limitation is also nutrient-dependent, and follows the Monod uptake kinetics model. All phytoplankton groups are limited by nitrogen, as nitrate and ammonium, and diatoms are additionally limited by silicate concentrations. Ammonium is preferentially utilized over nitrate, following the formulation of Gregg and Walsh (1992). Half-saturation constants are group-independent. The cyanobacteria component possesses a modest ability to fix nitrogen from the

water column, as is observed in the cyanobacterium *Trichodesmium* spp. (Carpenter and Romans, 1991). Nitrogen fixation is expressed as 0.001 the light-limited growth rate, and only applies when nitrate availability is $<1\ \mu\text{M}$. Fixed nitrogen is denitrified by the detrital component to prevent nitrogen accumulation in the model domain.

Typical sinking rates for the phytoplankton groups are computed by declaring representative individual sizes, and then using Stokes Law under typical oceanic conditions (Gregg, 2000). Modification of this rate can occur under circumstances deviating from the typical conditions, such as in extremely cold water where viscosities are large. Using Stokes Law, this effect is parameterized in terms of temperature. Simulation of grazing by the herbivore component is based on McGillicuddy et al. (1995). A temperature-dependence in grazing is enforced.

A radiative transfer model contains a treatment of the spectral and directional properties of radiative transfer in the oceans, and explicitly accounts for clouds. It contains an optical characterization of atmospheric and in-water optical constituents. The atmospheric radiative model is based on the Gregg and Carder (1990) spectral model for clear skies, and relies on Slingo (1989) for spectral cloud transmittance. It requires external monthly climatologies of cloud properties (cloud cover and liquid water path), surface pressure, wind speeds, relative humidity, ozone, and precipitable water. Computations are made only for the spectral range 350–700 nm (photosynthetically available radiation, or PAR), since the model is used to drive phytoplankton growth only, and only every 2 h to provide diurnal variability at an acceptable computational cost.

Oceanic radiative properties are driven by water absorption and scattering, and the optical properties of the phytoplankton groups. Three irradiance paths are enabled: a downwelling direct path, a downwelling diffuse (scattered) path, and an upwelling diffuse path. All oceanic radiative calculations include the spectral nature of the irradiance.

Nitrate and chlorophyll outputs from the climatologically forced model after a 4-year run indicate good correspondence with seasonal nitrate fields from in situ archives and monthly chlorophyll from the CZCS (Fig. 1). Seasonal nitrate data were obtained from NOAA/National Oceanographic Data Center (NODC)/Ocean Climate Laboratory (OCL) (Conkright et al., 1998a–c) and averaged over the model surface mixed-layer depth. Overall correspondence between the in situ data and the model is indicated with large concentrations in the high latitudes and equatorial upwelling regions, and low concentrations in the central ocean gyres. Similar correspondence is indicated with respect to model and CZCS chlorophyll.

Modifications to the existing model (Gregg, 2000) were (1) forcing by actual atmospheric conditions during the SeaWiFS era, rather than the monthly climatologies used previously, and (2) a parameterization of biological processes in sea ice. An overview of the coupled model interactions illustrates the application of monthly surface wind stresses, shortwave radiation and sea ice (re-analysis products from the NOAA/National Center for Environmental Prediction, NCEP), and sea surface temperature from the Reynolds optimal interpolation analyses (OISST: Reynolds and Smith, 1994) obtained from the GSFC/DAAC (Fig. 2). Unfortunately, actual cloud properties were not available yet for this period from the International Satellite Cloud Climatology Project, so we used monthly climatologies surface spectral irradiance (to drive phytoplankton growth). Also, shortwave radiation was not available for June 2000, so again climatology was used.

In this version biogeochemical processes in sea ice were parameterized. This adaptation was necessitated by lack of overwintering success by phytoplankton in the extreme northern and

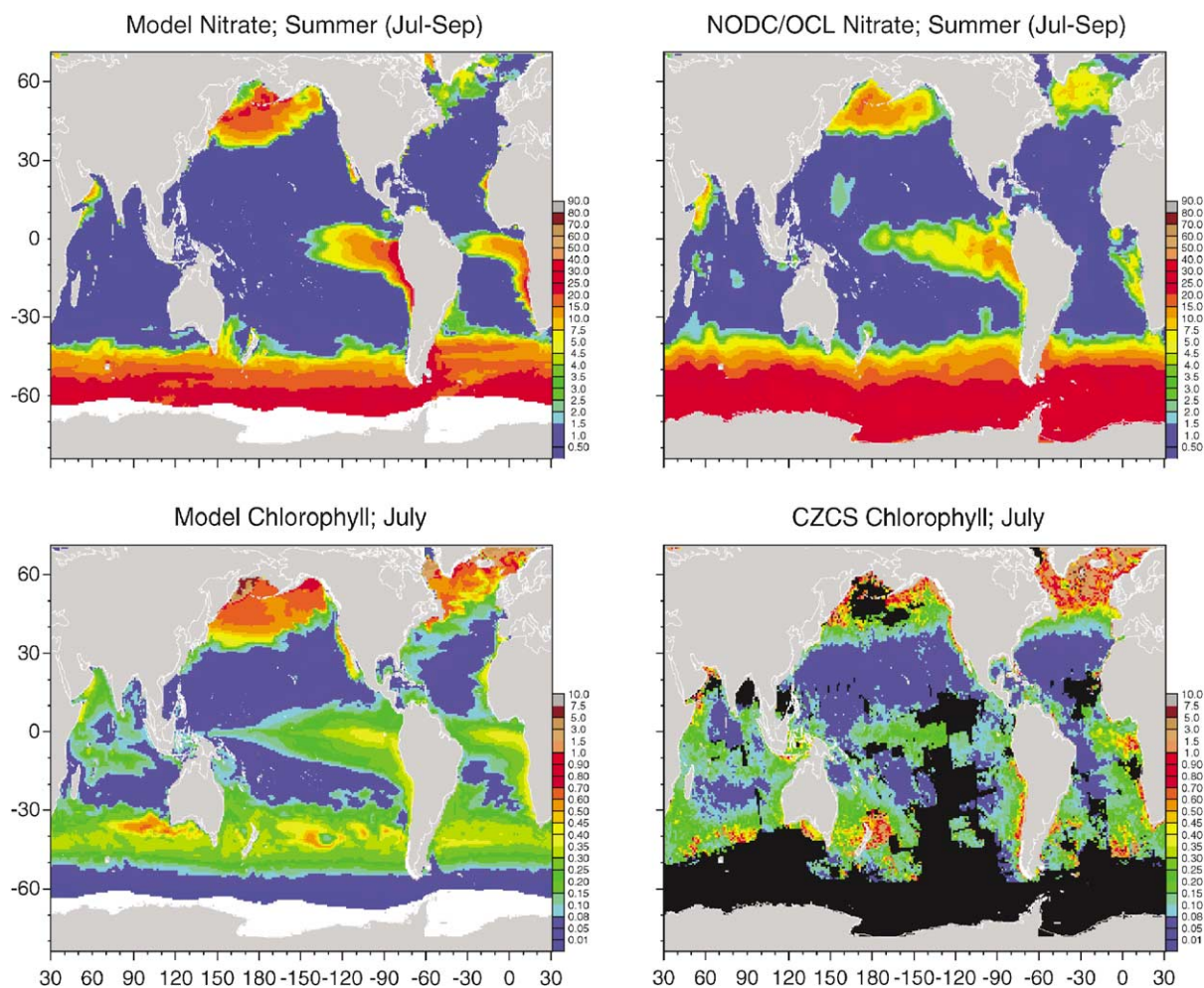


Fig. 1. Comparison of model nitrate and chlorophyll from a 4-year run using climatology for surface forcing with NODC/OCL nitrate (top), and CZCS chlorophyll (bottom). Model nitrate and chlorophyll represents the mixed layer mean, NODC nitrate is averaged over the mixed layer. This run produced the initial conditions for the comparison of interannual variability discussed in this paper. Missing data are shown in black.

southern ranges of the model, resulting in depletion of populations. In the previous model, phytoplankton populations became so depleted in the local winter that they could not recover during the growing season. In nature, phytoplankton exist in sea ice over winter, and then enter the ocean upon ice melt (Smith and Nelson, 1986), a process known as seeding. The simple parameterization applied here was to cease all biogeochemical processes in the presence of sea ice, and then resume when the ice disappears. The activity was modified by the percentage of sea ice present in a model grid cell. This is a conservative parameterization, since phytoplankton actually grow in sea ice in local spring when sufficient irradiance becomes available (Robinson et al., 1998; Arrigo et al., 1995; Arrigo and Sullivan, 1994). Advection, diffusion, and convection of biogeochemical constituents is allowed to continue despite the presence of sea ice.

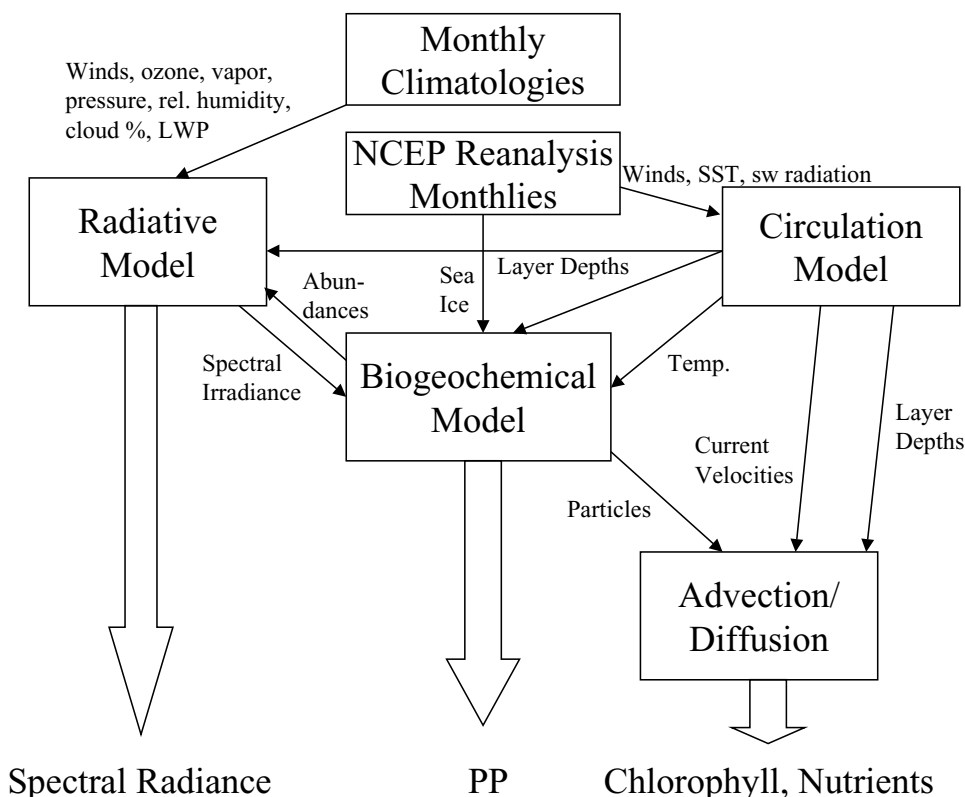


Fig. 2. Diagrammatic representation of the coupled circulation, biogeochemical, and radiative model of the global oceans. Monthly climatological wind and atmospheric optical properties are used to produce spectral irradiance fields. Near-real-time monthly means of wind stresses, SSTs, shortwave radiation, and sea ice are used to drive the circulation and biogeochemical fields for the SeaWiFS record. Outputs from the model are spectral upwelling radiance, primary production (which is an explicit calculation derived from the growth functions), chlorophyll abundances for each of the phytoplankton groups, and nutrients (nitrate, ammonium, and silicate). LWP is cloud liquid water path.

As in Gregg (2000), the OGCM was run for 5 years with climatological wind stresses, SST, and surface shortwave fluxes. Then the biogeochemical model was initialized with homogeneous fields of diatoms, chlorophytes, and cyanobacteria each set at 0.05 mg m^{-3} chlorophyll concentrations. Initial nitrate and silicate fields were taken from Conkright et al. (1994) annual means. The coupled model was run for 4 years with climatological surface wind stresses, SST, shortwave fluxes, sea ice, and atmospheric optical constituents to avoid initialization effects and achieve steady state. Finally the model was run from January 1997 to June 2000 using actual wind stresses, SST, shortwave radiation, and sea ice fields for the months and years in question.

2.3. Analysis of results

The SeaWiFS chlorophyll data were compared to model surface mixed-layer chlorophyll outputs seasonally and throughout the September 1997 to June 2000 record. The results were

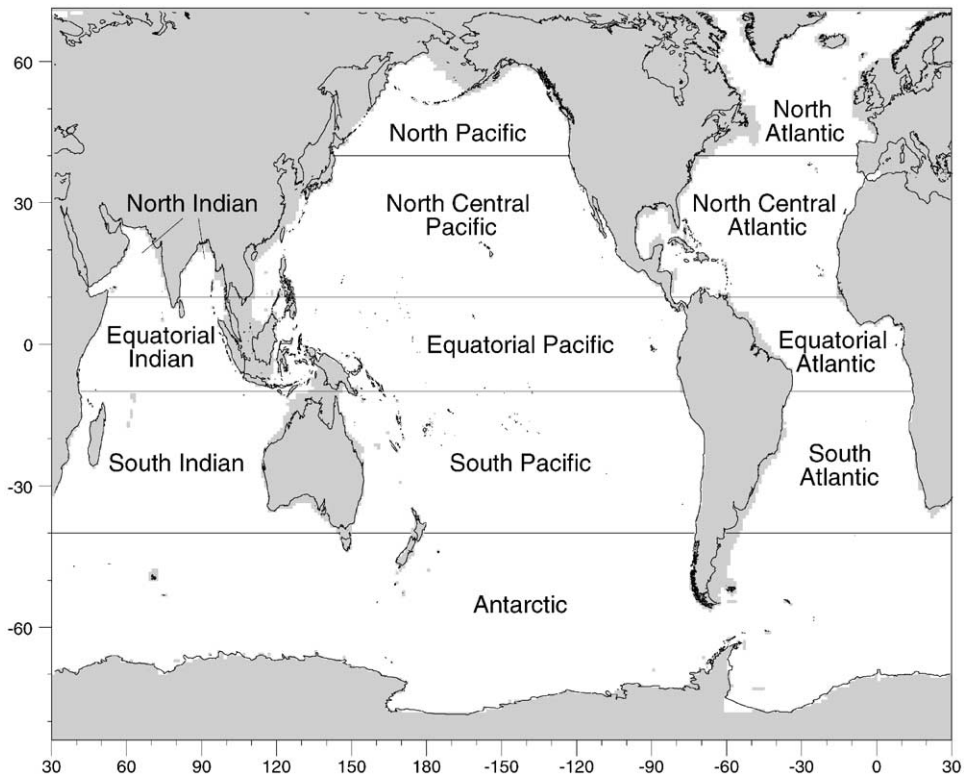


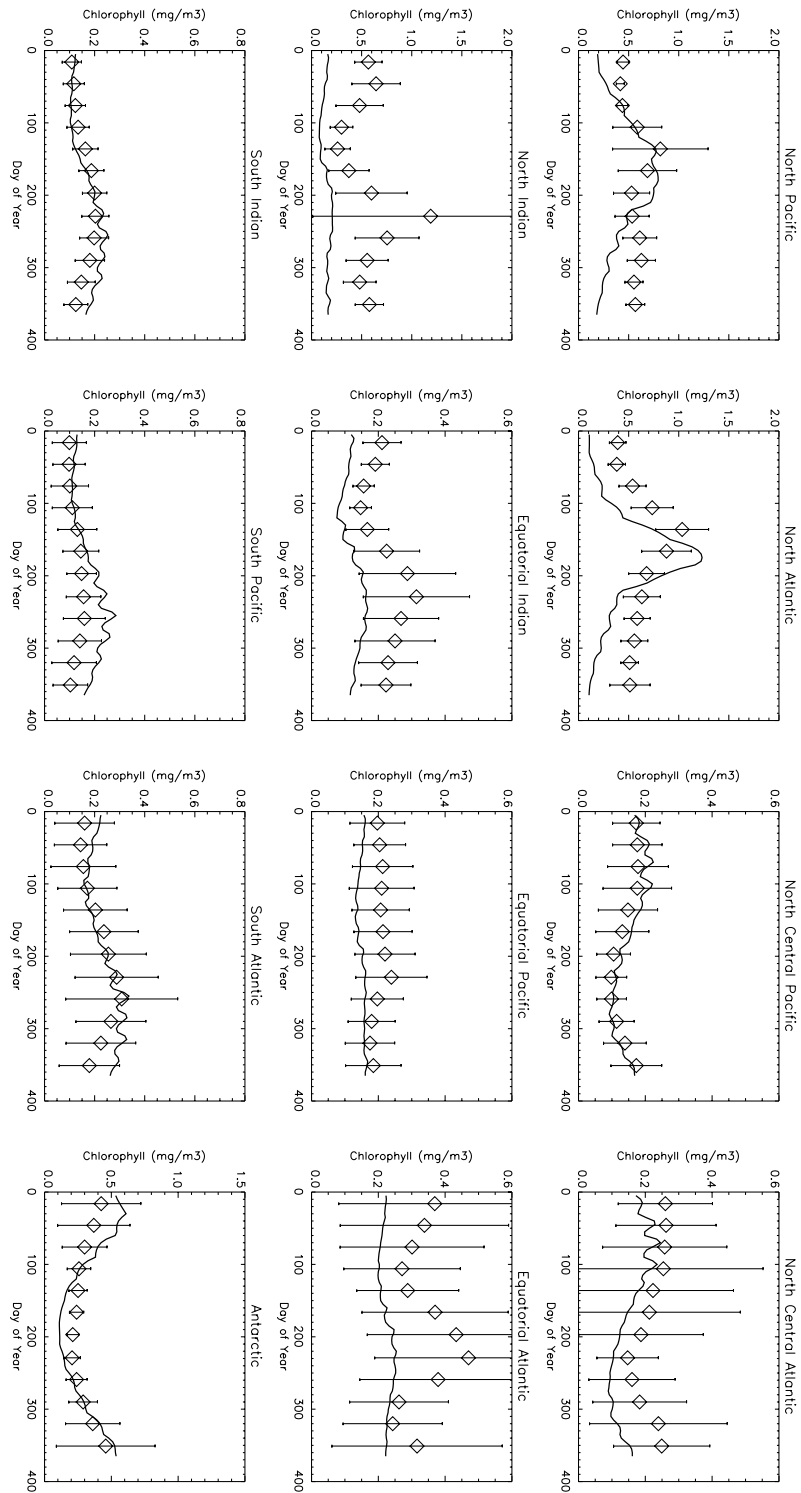
Fig. 3. Location of the 12 major oceanographic basins in the global ocean.

analyzed on basin scales and as a comparison of images which represents a synoptic scale analysis. Basin definitions (Fig. 3) are derived from standard descriptions commonly in use (e.g., Conkright et al., 1994), with additional equatorial, or tropical, subdivisions in each major ocean from -10° to 10° latitude. Antarctic is defined as southward of -40° .

3. Results and discussion

3.1. Seasonal comparison of total chlorophyll in the SeaWiFS record

The SeaWiFS record of chlorophyll concentrations from September 1997 to December 1999 was averaged monthly to produce an illustration of seasonal distributions. Similarly, total chlorophyll outputs from the model were averaged daily over the same period. The comparison shows general correspondence between SeaWiFS and model-computed total chlorophyll (Fig. 4). Regions of low and high chlorophyll were matched, and the general characteristics of the seasonal cycle were in agreement. The high-latitude regions, the North Atlantic and Pacific Oceans, and the Antarctic Ocean were characterized by a very wide seasonal range of chlorophyll, with a prominent and large local spring/summer bloom and a large die-off in local winter. Mid-latitude regions (North Central Pacific and Atlantic, South Indian, Pacific, and Atlantic basins) were

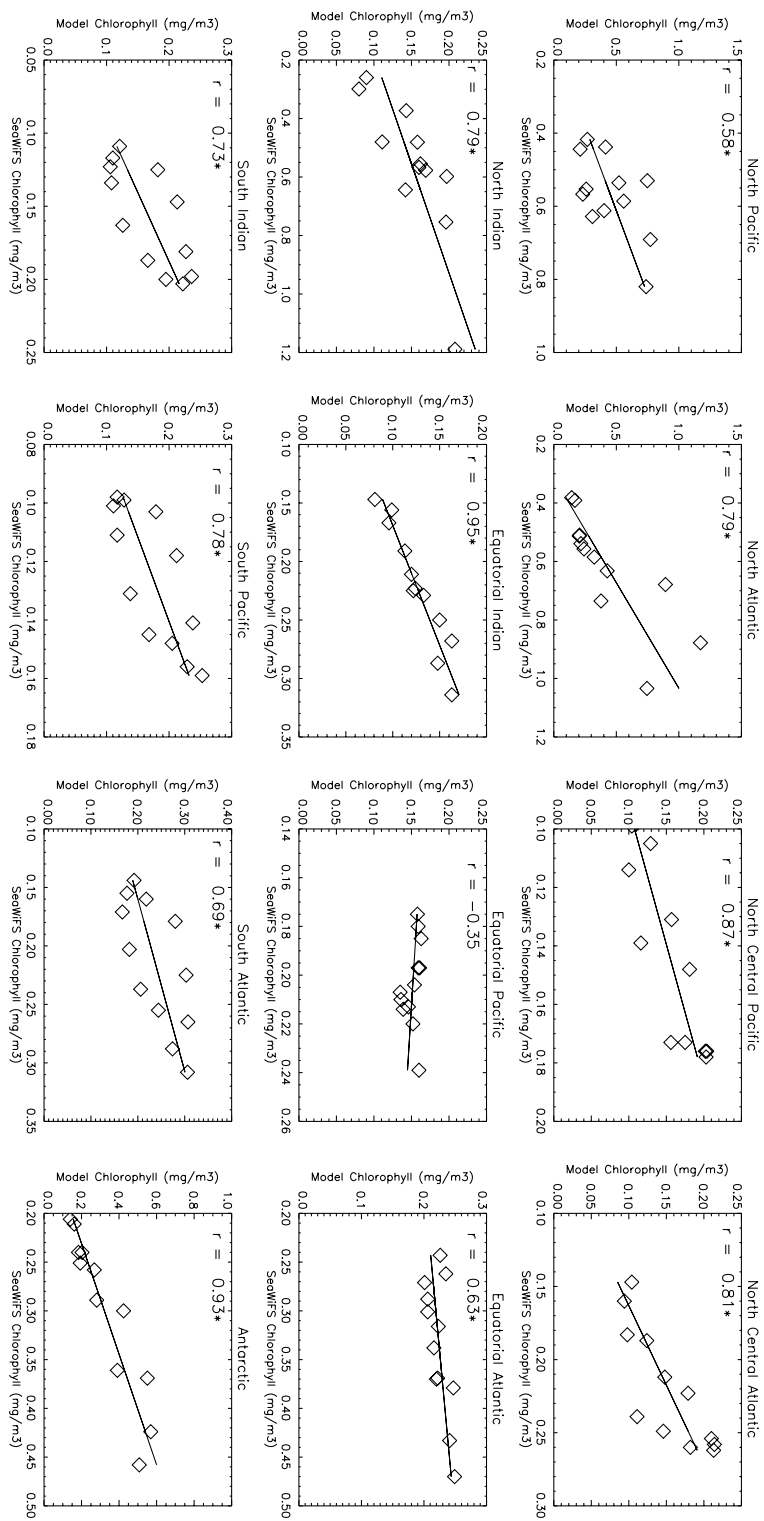


characterized by a much smaller seasonal signal, with local winter producing maximum values. The equatorial Pacific had virtually no seasonal signal in either the model or SeaWiFS. The equatorial Atlantic had a prominent seasonal signal, with two maxima (boreal summer and boreal winter) and two minima (boreal spring and fall) in SeaWiFS. The boreal summer maximum corresponds to the maximum upwelling season (Signorini et al., 1999; Monger et al., 1997), and was captured by the model but not as intensely. The boreal winter maximum corresponds to the season of maximum discharge from the Congo River, which is not simulated by the model. The model agreed with the boreal spring minimum, but did not exhibit a fall minimum, probably because this is an artifact of the secondary maximum due to Congo River discharge. There was agreement in the amount of chlorophyll during this season, however. The tropical Indian Ocean was lowest in mid-spring and highest in summer, which agreed with the model results, but again the model appeared to underestimate the magnitude. The North Indian Ocean seasonal signal was clearly dominated by the northwest monsoon in mid-winter, the even larger southwest monsoon in summer, and a minimum in chlorophyll associated with the inter-monsoon period. The model seasonal trends were in agreement with these results, but it underestimated the high chlorophyll values at the monsoon peaks. The southwest monsoon is a period of intense upwelling that produces elevated chlorophyll, but high winds associated with the monsoon also produce overlying absorbing aerosols that confound the SeaWiFS atmospheric correction algorithms and produce an overestimate of chlorophyll. Still, the model did not appear to represent the extent of upwelling, which may be due to the absence of topographic and/or coastal influences, or inadequate model spatial resolution.

Correlation analysis of these seasonal trends indicated that the model was statistically positively correlated with every region at the 95% confidence interval, except in the equatorial Pacific (Fig. 5). The seasonal signal is very small in this basin, as indicated by both the model and SeaWiFS, which is responsible for the poor correlation, since chlorophyll concentrations are in general agreement (Fig. 4).

Although the model exhibited an ability to simulate the seasonal distributions of chlorophyll as compared to SeaWiFS, there were some significant differences in timing and magnitude. In the North Pacific and Atlantic, the spring bloom peak occurred in the model in June (Fig. 4). In SeaWiFS the bloom occurred in May in both basins, although it lingered through June. This represents a departure from the CZCS climatology, when the peak occurred in June in both basins, although the North Pacific May values were nearly equal to June (Fig. 6). In the model the bloom resulted from increased surface irradiance and mixed layer shoaling. Coupled with prevalent nutrients from winter mixed-layer deepening and entrainment, this produced irradiance levels in the surface layer conducive to very large growth, which fully developed in June. The higher May monthly mean chlorophyll in the SeaWiFS North Pacific basin was mostly due to localized high values around the northern and western rim of the basin (Fig. 7), bordering Alaska and Kamchatka. These areas can contain residual sea ice from the previous winter that may

Fig. 4. Comparison of model-generated mean chlorophyll (solid line) with monthly mean SeaWiFS chlorophyll by oceanographic basin, to illustrate seasonal variability over the SeaWiFS record from September 1997 to December 1999. SeaWiFS monthly means were derived by averaging the monthly means over the nearly 3-year record. Model means were averaged daily over the same period. Error bars on the SeaWiFS chlorophyll means represent one-half the SeaWiFS standard deviation.



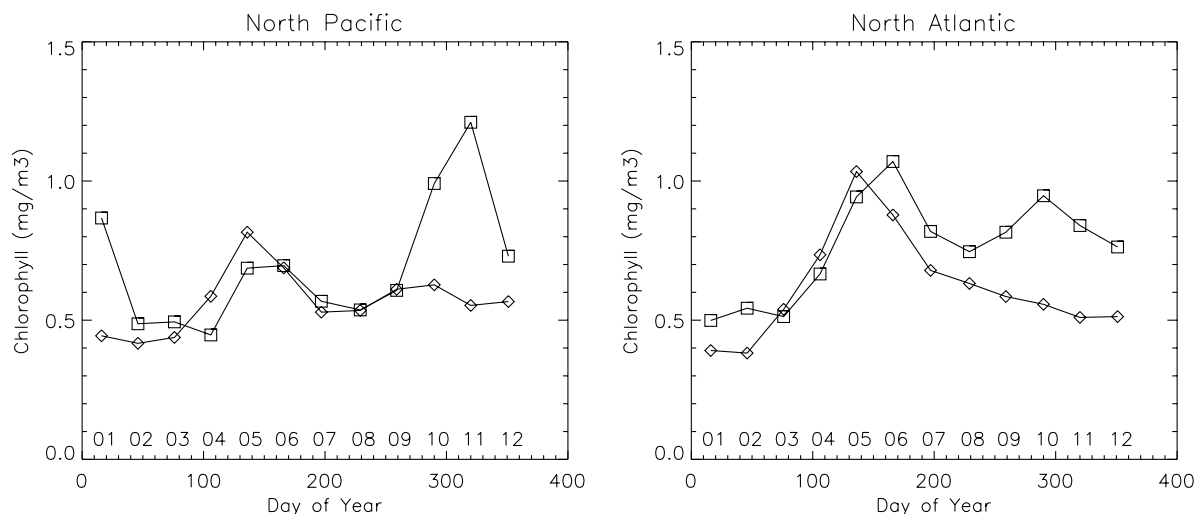


Fig. 6. CZCS climatological monthly mean chlorophyll (rectangles) for the North Pacific and North Atlantic basin, and SeaWiFS monthly means (diamonds). Months are indicated above the abscissa.

confuse the SeaWiFS algorithms. The problem was less apparent in CZCS data (Fig. 7), possibly because of sampling bias, better thresholds for ice and clouds, or other differences in algorithms. The more pelagic portions of the North Pacific exhibited more extensive blooming in June than May (Fig. 7), along with reduced chlorophyll concentrations near the rim. In the North Atlantic, the higher monthly mean in May was mostly due to large values in the Labrador Sea (Fig. 7). This is one of the coldest regions in the model domain, and does not develop a bloom in the model until June when accumulated solar heating can produce a shallower mixed layer. Again this region contains sea ice well into the spring, and SeaWiFS data may be affected by its presence. The CZCS did not appear as affected by Labrador Sea values.

The North Pacific also exhibited a pronounced fall bloom in SeaWiFS data that was not present in the model (Fig. 4). The CZCS climatology exhibited an even more pronounced feature (Fig. 6). Yoder et al. (1993) suggested that CZCS observations in the autumn above 40°N were unreliably high. While there may be bias associated with limited sampling and increasing solar zenith angle, the dynamics producing a fall bloom (convective overturn and replenishment of nutrients) are well-grounded in physical and biogeochemical principles. In the model nutrient replenishment was inadequate to compensate for diminished irradiance availability, especially given the deeper mixed layer. In reality, there may be influences related to eddy-forced isopycnal adjustment (e.g., Siegel et al., 1999) or diurnal variability of mixed-layer depths. The effect is not as large in SeaWiFS as in the CZCS, suggesting that the grossly large fall bloom in the CZCS is due to algorithm, sensor, and sampling problems, and the smaller bloom observed by SeaWiFS may be more realistic.

Fig. 5. Correlation of basin-scale mean model chlorophyll values with SeaWiFS. The solid line indicates the best-fit, and the correlation coefficient is indicated. An asterisk indicates that the correlation is significantly positively correlated at the 95% confidence level. The probability value to establish statistical significance is 0.576. The equatorial Pacific does not indicate positive correlation because of the lack of seasonal variability.

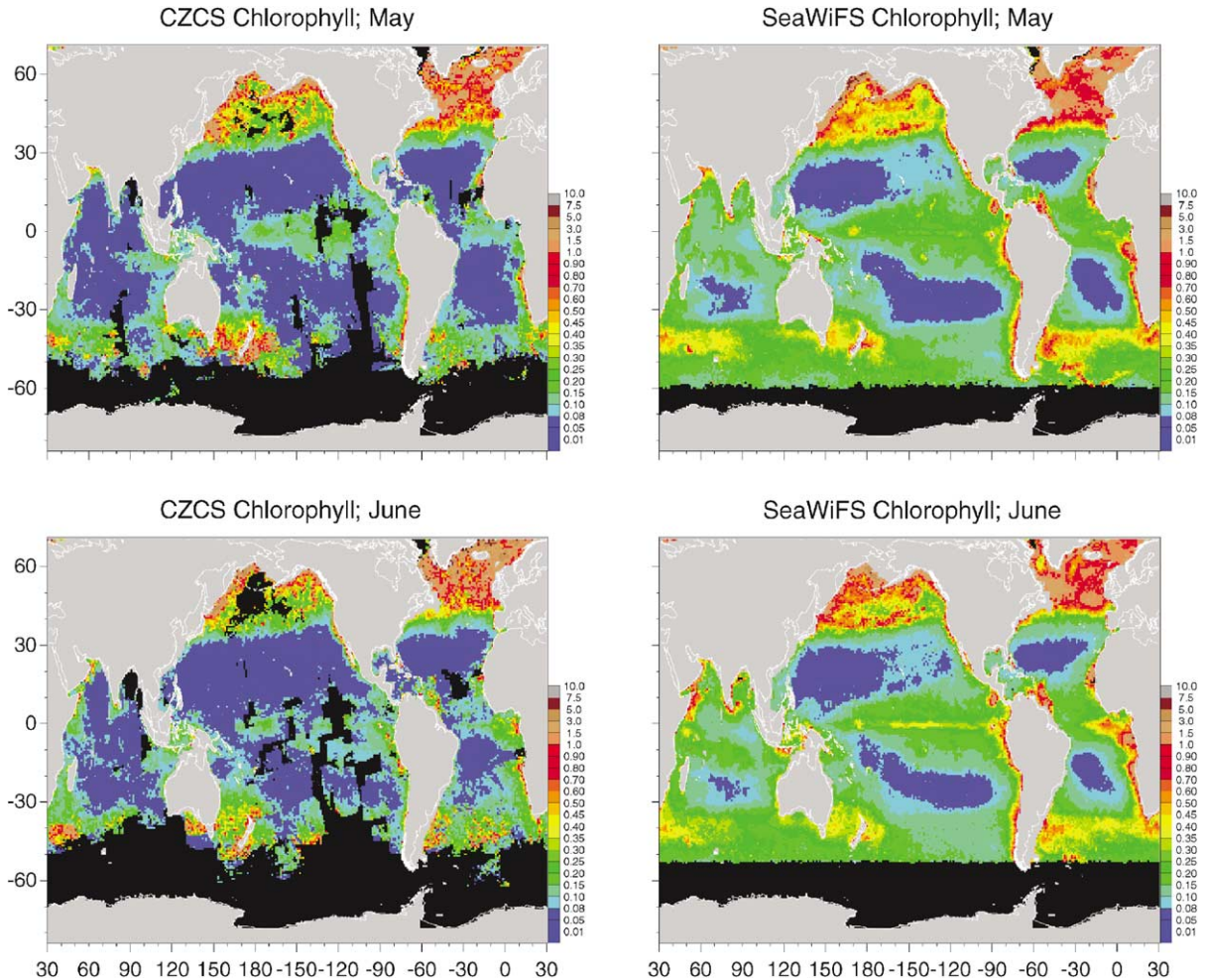
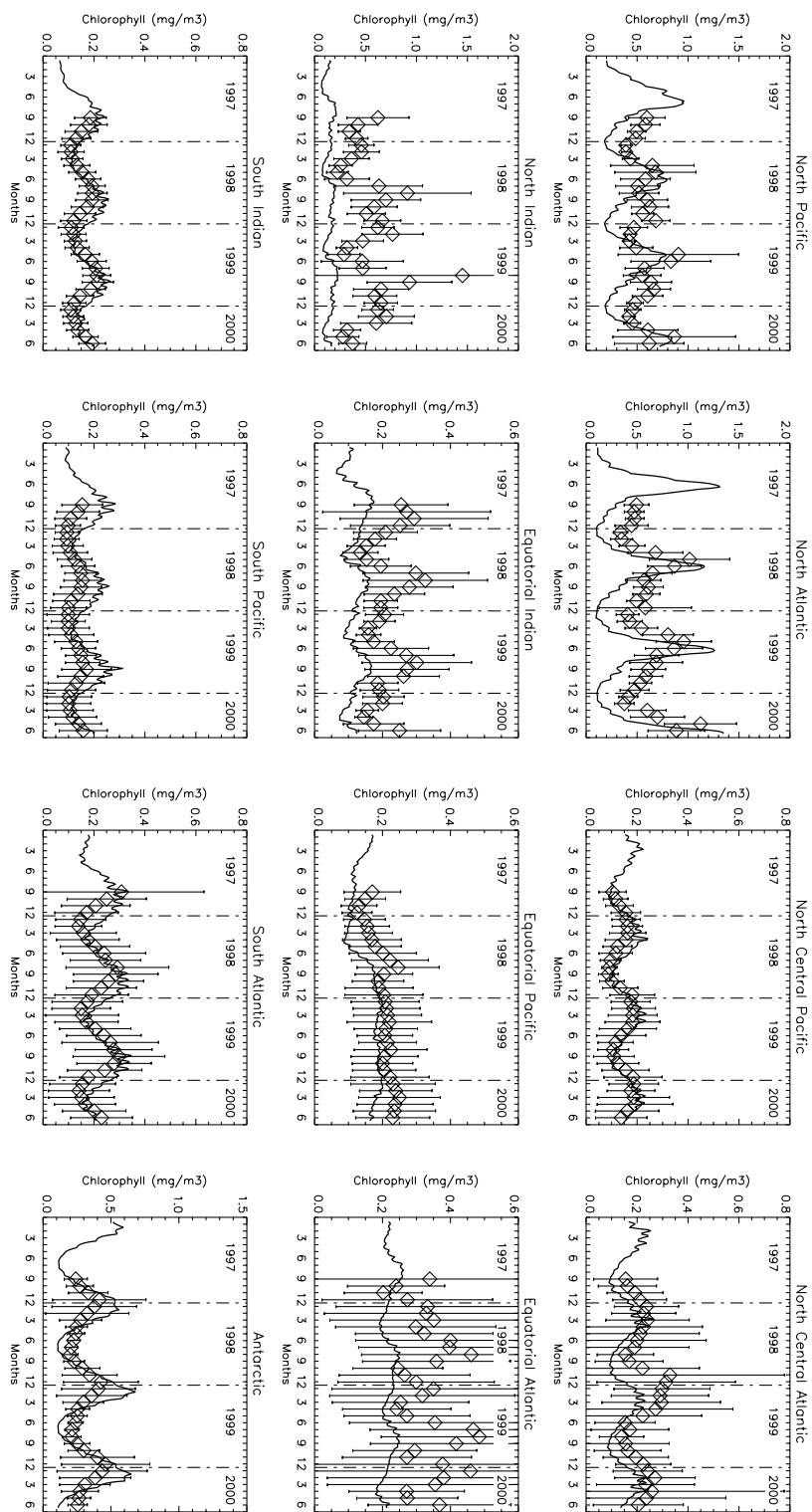


Fig. 7. Comparison of climatological monthly mean CZCS and SeaWiFS chlorophyll data for May and June. Color bar on the right indicates chlorophyll as mg m^{-3} . Land and non-active coastal areas are shown in gray, and missing data are shown as black.

3.2. Interannual comparison of total chlorophyll in the SeaWiFS record

The nearly 3-year SeaWiFS chlorophyll record (September 1997 to June 2000) investigated here was generally dominated by the seasonal signal, but interannual variability was also readily apparent (Fig. 8). Perhaps the most dominant event since the launch of SeaWiFS was the record El Niño and La Niña events in the tropical Pacific Ocean. The El Niño was underway in

Fig. 8. Comparison of model daily chlorophyll (solid line) with monthly mean SeaWiFS chlorophyll by oceanographic basin for the nearly 3-year SeaWiFS record from September 1997 to June 2000. Error bars on the SeaWiFS chlorophyll means represent one-half the SeaWiFS standard deviation.



September 1997 when SeaWiFS was launched, and continued (as indicated by anomalously high surface temperatures) until May 1998. Temperatures exceeded 4° above normal during the 1997–1998 event (Murtugudde et al., 1999). The high surface temperatures were the result of a series of eastward-propagating Kelvin waves, which in turn were induced by changes in wind patterns in the tropical Pacific (McPhaden and Yu, 1999; McPhaden, 1999). These Kelvin waves suppressed the normally present upwelling conditions, produced a deepening of the thermocline, and reduced the supply of nutrients to the surface (McPhaden and Yu, 1999; Chavez et al., 1998). The result was vastly reduced chlorophyll concentrations. Low chlorophyll concentrations were readily apparent in the SeaWiFS tropical basin means from launch until early 1998 (Fig. 8). Similar low chlorophyll was represented in the model basin means. However, there were some discrepancies between the computed response to El Niño and the actual response as indicated by the SeaWiFS observations. SeaWiFS reached a minimum in chlorophyll in December 1997 and apparently began to recover through early 1998. The model obeyed the OISST record, which showed that the El Niño did not end until May 1998. Murtugudde et al. (1999) suggested that local wind bursts beginning in March 1998 produced a local bloom in SeaWiFS data near 165°E . The monthly mean winds used in the model were unable to simulate this type of localized event. One of the most notable features of the midst of the El Niño was the prominent expression of a band of low chlorophyll in SeaWiFS just north of the equator, corresponding to the location of the equatorial counter current. The expression of this band of low chlorophyll was readily apparent in the model (Fig. 9).

The La Niña condition, prevalent in the equatorial Pacific from May 1998 to the end of the record under investigation here (June 2000), was represented in the SeaWiFS data and the model (Fig. 8). Both indicated elevated chlorophyll concentrations, resulting from enhanced upwelling and supply of nutrients to the surface. Both indicated about a factor of 2 increase from the low point of the El Niño to the La Niña (Fig. 8). Re-establishment and intensification of upwelling conditions due to La Niña are shown in Fig. 10.

The expression of the El Niño in the tropical Indian Ocean was also one of the significant interannual signals observed by SeaWiFS. Anomalous upwelling in the eastern tropical Indian Ocean was present in both the SeaWiFS data and the model in December 1997 (Fig. 9). This upwelling was induced by abnormally high wind stresses, which produced abnormally low SST indicative of upwelling. In the model and SeaWiFS, the wind stresses slowed beginning in December 1997 and resulted in a steady reduction of surface chlorophyll in the equatorial Indian basin until the end of the El Niño in May 1998, when a more normal seasonal cycle began to assert itself. The departure of model chlorophyll from SeaWiFS in the boreal summer of 1998 and 1999 may have been influenced by atmospheric correction difficulties in SeaWiFS associated with dust plumes accompanying the high winds of the southwest monsoon. Massive areas of the Arabian Sea failed the aerosol optical thickness criterion for SeaWiFS during these periods (Fig. 10). The absorbing nature of these aerosols produces erroneously high estimates of derived chlorophyll in the correction procedures. Algorithm failure was apparent in the equatorial Indian monthly means, and excessively large chlorophyll values are an expected result in the presence of sub-threshold aerosol optical thicknesses. Most of the increase in chlorophyll in the equatorial Indian in July and August occurred on the western side, closest to the dust source (Fig. 10). Similar large chlorophyll concentrations were retrieved from SeaWiFS during these months for the North Indian and equatorial Atlantic Oceans,

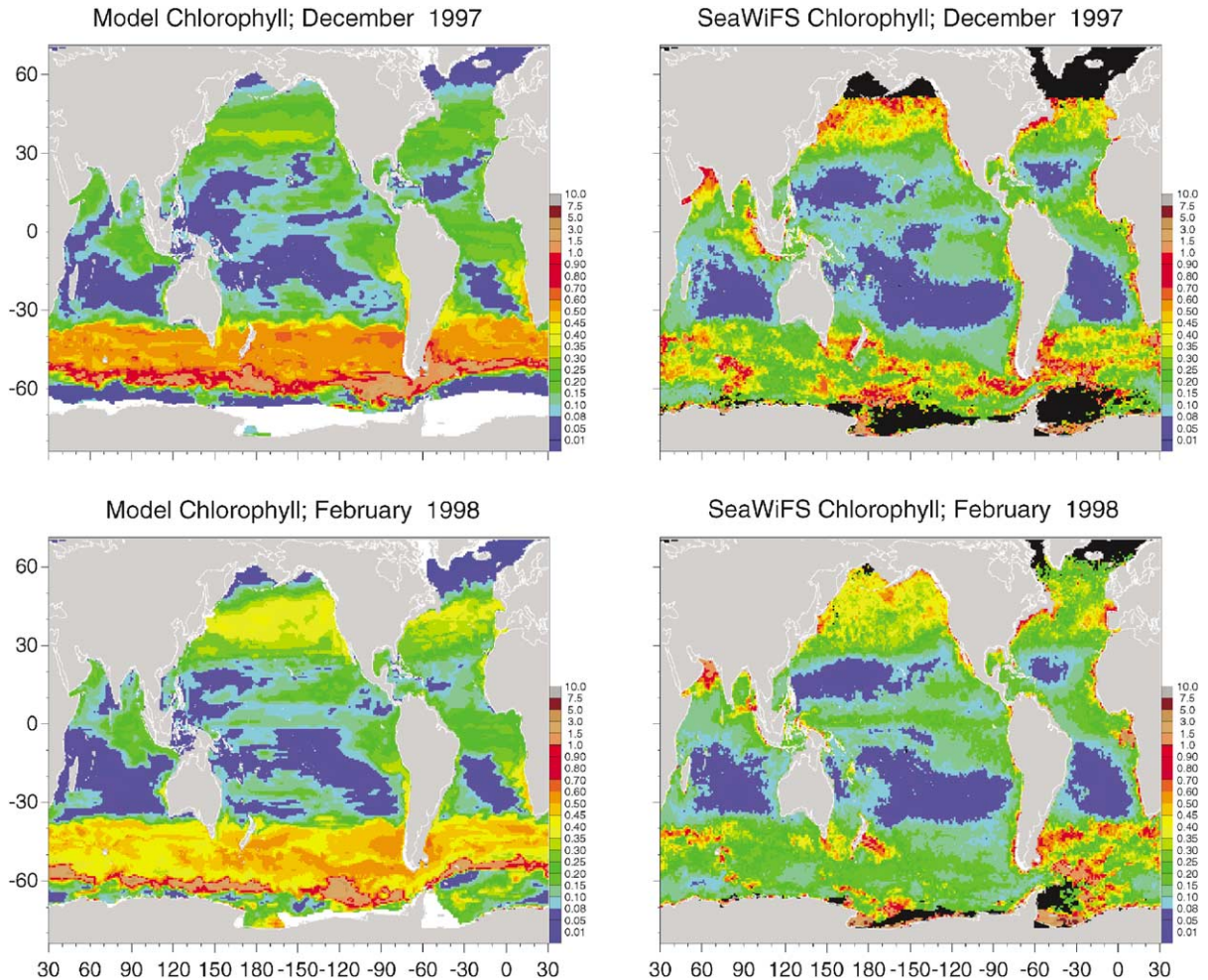


Fig. 9. Top: Mean monthly model chlorophyll for December 1997 compared with SeaWiFS data. Bottom: February 1998. This shows the evolution of the El Niño in the equatorial Pacific and Indian Oceans. Note suppressed chlorophyll concentrations in the equatorial Pacific and increased concentrations in the eastern equatorial Indian. Color bar on the right indicates chlorophyll as mg m^{-3} . Land and non-active coastal areas are shown in gray, missing data are shown as black, and sea ice fields are shown in white.

suggesting a similar phenomenon. Some of the effect most likely resulted from upwelling induced by the southwest monsoon, but it is difficult to quantify. The model may be inhibited from exhibiting the large dynamic range in chlorophyll because of the lack of topographic and coastal influences, or possibly inadequate spatial resolution. Another possibility is the inadequate representation of vertical mixing due to the use of monthly mean winds.

A time series of surface nitrate distributions (Fig. 11) illustrates the dramatic effects of El Niño and La Niña. Nitrate concentrations were low in November 1997 in the tropical Pacific, but upwelling was strongly indicated in the eastern tropical Indian basin. By May the nitrate depletion

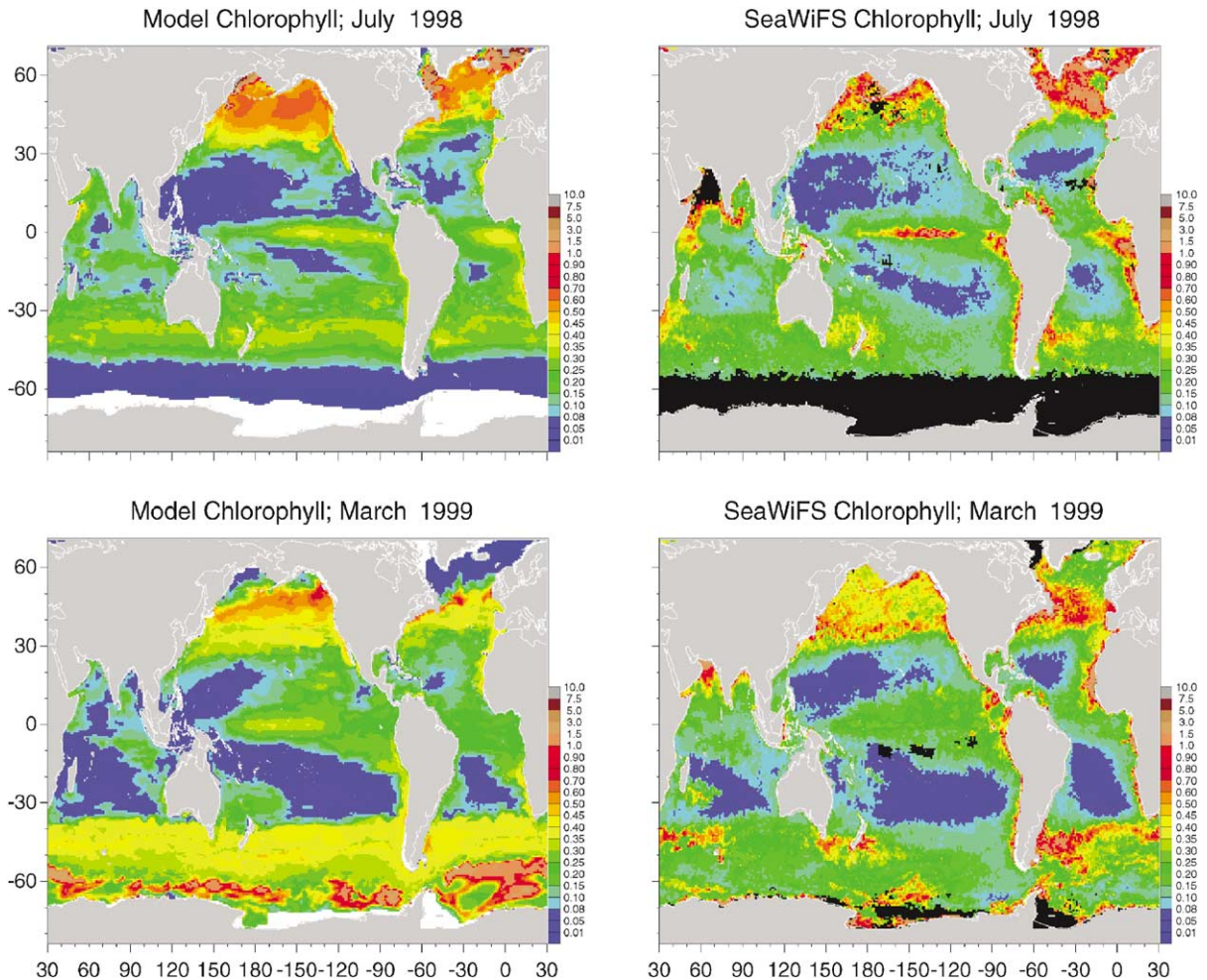


Fig. 10. Top: Mean monthly model chlorophyll for July 1998 compared with SeaWiFS data. Bottom: March 1999. By July 1998 the La Niña is well-established and is indicated by high chlorophyll concentrations in the equatorial Pacific. In March 1999 an intense bloom of chlorophyll appears off the coast of Mauritania in the North Central Atlantic in the SeaWiFS data. The model indicates this but not as intensely. This sequence of images also illustrates seasonal variability. The vestiges of the austral summer bloom in the Antarctic are clearly apparent in the model, and sometimes agrees with SeaWiFS, but appear to overestimate especially in the southeast portion of the Pacific sector.

in the tropical Pacific reached its maximum, and within one month reversed, indicating the onset of La Niña. Murtugudde et al. (1999) observed a 6°C change in temperature between May and June 1998. By September 1999 La Niña was firmly entrenched in the tropical Pacific. Chavez et al. (1999) measured 0.05 μM nitrate at 0° 155°W in November 1997, which was lower than the corresponding model value of 0.5 μM , but which represented a significant departure from a normal value of about 5 μM .

The North Central Pacific Ocean appeared to exhibit interannual variability related to the El Niño (Fig. 8), with lower peak values in the SeaWiFS data in winter/spring 1998 than in 1999.

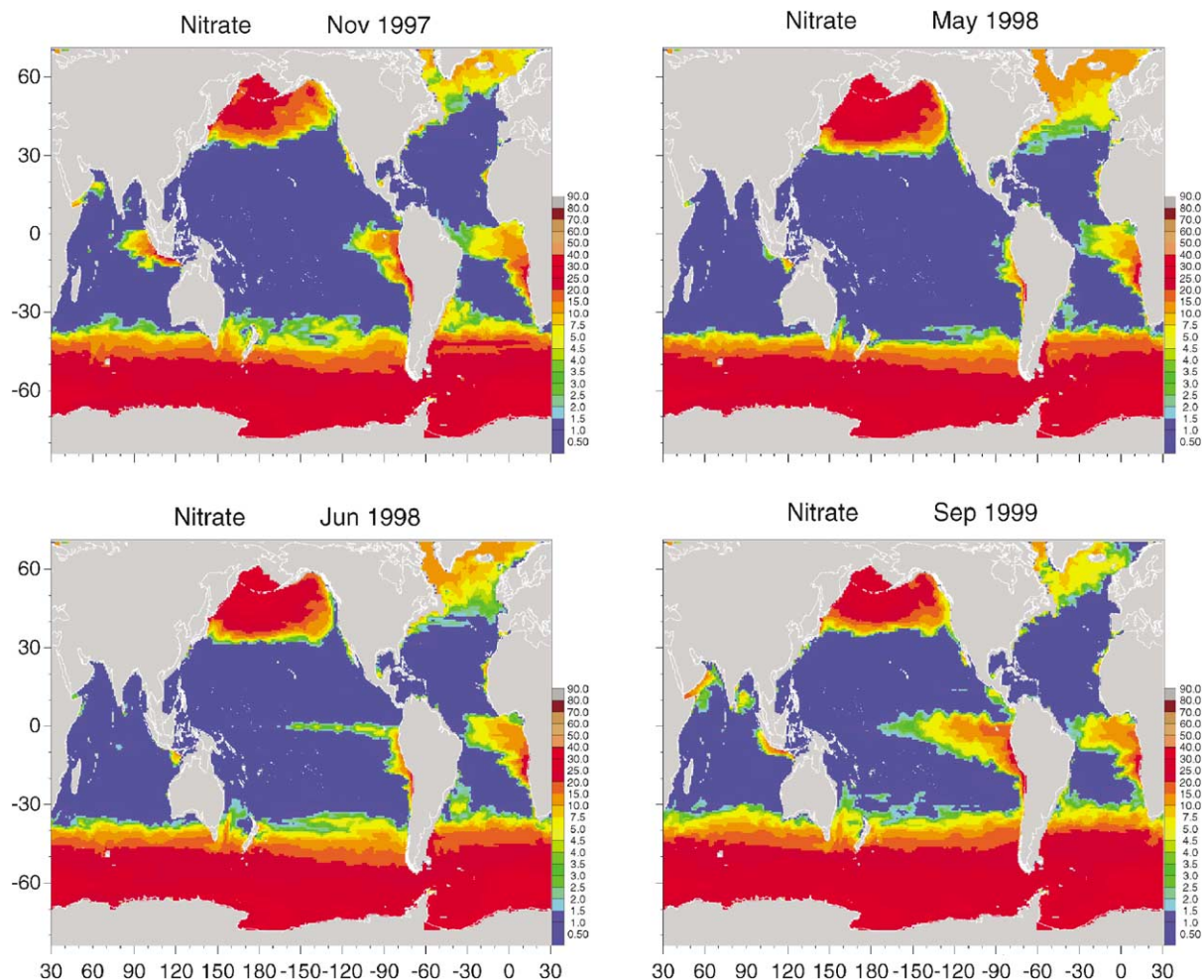


Fig. 11. This sequence of images illustrates the dramatic effects of El Niño and La Niña in model surface nitrate concentrations. In November 1997 high nitrate values in the eastern equatorial Indian occurred as a result of intense upwelling. Nitrate concentrations continued to diminish through May 1998 in the tropical Pacific, and then began to re-establish upwelling conditions in June 1998 as the La Niña developed. By September 1999 the La Niña was fully established. Seasonal variability was also apparent in the sequence. Note the exhaustion of nitrate in the North Pacific and Atlantic in November 1997 and September 1998, as the result of phytoplankton growth in the boreal summer. Replenishment occurred by May 1998. A much smaller seasonal signal was also apparent in the southern ocean. Color bar at right indicates units of μM .

This was accompanied by anomalously high SSTs along the California coast in spring 1998, which was indicative of reduced upwelling. The model indicated reduced upwelling along the California coast in spring 1998 as well, but overall the basin mean values in the model did not exhibit effects related to the El Niño.

The North Pacific basin also exhibited interannual variability during the nearly 3-years of SeaWiFS chlorophyll data collection under investigation (Fig. 8). The May spring bloom was

Table 1
Mean depth of surface mixed layer (m) in the North Pacific in spring

	1998	1999	2000
March	92.2	112.7	109.2
April	93.4	83.0	85.9
May	64.7	42.4	24.5
June	21.6	23.7	19.8

larger in 1999 and 2000 in the SeaWiFS record than in 1998. The model also exhibited larger blooms in 1999 and 2000, and matched the timing of the peak (May), but showed an extended bloom in 1998 with a maximum in June (Fig. 8). The shift to the May bloom and the larger magnitudes in the model was the result of the depth of the mixed layer (Table 1) and the rate of mixed-layer shoaling. In 1998 the mixed layer shoaled at a rate of about 9.2 m month^{-1} reaching a depth of 65 m in May, compared to $23.4 \text{ m month}^{-1}$ in 1999 and $28.2 \text{ m month}^{-1}$ in 2000. Shallower mixed layers in May in 1999 and 2000 (Table 1) provided more average irradiance in the mixed layer and enabled phytoplankton to maximize light-limited growth. The accelerated shoaling did not allow herbivore populations time to keep up with the phytoplankton, and the phytoplankton grew until nutrients were exhausted, with less cropping. The reduced June chlorophyll concentrations in the model were a direct result of nutrient depletion that occurred in May in both 1999 and 2000, and was in agreement with SeaWiFS. In 1998, the slow development of shallow stratification allowed herbivore populations to keep up with the phytoplankton, preventing the quick exhaustion of nutrients, and thus reducing the overall bloom magnitude but also spreading out the period of high chlorophyll over three months.

As in the North Pacific, the North Atlantic spring bloom also peaked in May in the SeaWiFS record, but the model consistently showed a June maximum (Fig. 8). The 1999 May bloom in SeaWiFS was lower than in 1998, as it was in the model. In the model the mean mixed-layer depth was 57 m in 1999 compared to 33 m in 1998, which explains the interannual difference. However, SeaWiFS chlorophyll increased in May 2000, while model chlorophyll decreased due to an even deeper mixed layer of 61 m. The North Atlantic SST was 0.2° cooler in 2000 than in 1999, with twice the mean wind stress, which produced the deep mixed layer and reduced chlorophyll concentrations in the model.

The model tracked the SeaWiFS chlorophyll record in the North Central Atlantic, except for a 7-month period beginning in October 1998 and lasting until April 1999, when elevated SeaWiFS values predominated (Fig. 8). After this time the SeaWiFS data fell back to agreement with the model. The elevated SeaWiFS data for the basin were caused by very high chlorophyll values off the coast of Mauritania during this period (Fig. 10). The mean chlorophyll in the anomalous area was 2.8 mg m^{-3} for SeaWiFS in November 1998 compared to 0.17 for the model and 0.7 for the CZCS climatology. SST data for this period were actually warmer than in 1997 and 1999, and wind stresses were similar to 1997 and 1999 with similar directionality. This suggested that upwelling of nutrients was not the cause of the high SeaWiFS chlorophyll off Mauritania. The model did not exhibit an unusual response in late 1998, supporting the external evidence. This

suggests the possibility of a Saharan dust episode producing inaccurate SeaWiFS chlorophyll data.

However, conditions began to change by January 1999. Exceptionally strong southwestward wind stresses and reduced SSTs (1.1°C cooler in February 1999 than in 1998), suggesting anomalous upwelling, kept SeaWiFS chlorophyll high in the Mauritania region in boreal winter 1999. The model also reflected these conditions with simulated values 40% higher in 1999 than in 1998, although still well below the SeaWiFS estimates. Thus it appears that a Saharan dust outbreak in boreal fall 1998 gave way to anomalous upwelling in winter 1999, and together produced the 7-month elevated chlorophyll signal in SeaWiFS.

The equatorial Atlantic exhibited wide fluctuations in seasonal and interannual SeaWiFS data that were not matched in magnitude by the model (Fig. 8). SeaWiFS chlorophyll in boreal summer exceeded the model estimates by about a factor of 3, although the model also exhibited strong upwelling patterns (Fig. 12) that are expected in this season (Signorini et al., 1999; Monger et al., 1997). The summer 1999 basin mean was about 10% higher than in 1998, but was unaccompanied by stronger wind stresses or lower SSTs that would indicate increased upwelling. The region of high chlorophyll extended further west along the equator in summer 1999 than in summer 1998, but it was accompanied by larger chlorophyll in the Gulf of Guinea as well as in the Amazon River plume (Fig. 12). Summer rainfall in the African Sahel was the third highest since 1962 (Le Comte, 2000), producing flooding in the Niger River drainage area, which may contribute to elevated chlorophyll in the SeaWiFS record, especially in the Gulf of Guinea area. Secondary maxima occurring in SeaWiFS in boreal winter (Fig. 8) were most likely due to the Congo River, which reaches its maximum discharge at this time of year. The basin mean in boreal winter 2000 exceeded that in 1998 and 1999 by 27%, which corresponds to a record flood of the Congo River beginning in December 1999 (Le Comte, 2000). Enhanced chlorophyll values were readily apparent in SeaWiFS data near the Congo mouth during this time (Fig. 12). The model did not track the wide interannual variability of the SeaWiFS record, and appeared to stay on the seasonal course, although it was always within the SeaWiFS standard deviation. River influences are not included in the model, and so discrepancies between the two chlorophyll estimates cannot be expected in times of exceptional river discharges. However, it is likely that much of the evidence of rivers in the SeaWiFS data is not actually chlorophyll, but rather colored dissolved organic matter (CDOM), which is typically very abundant in tropical rivers (McClain et al., 1997).

The Southern Hemisphere basins appeared to exhibit very little interannual variability in either the SeaWiFS or model representations of chlorophyll, and the two were in overall agreement (Fig. 8). The model tended to underestimate SeaWiFS concentrations in the austral winter in the Antarctic. In the model, low irradiances and deep convective mixing inhibit primary production and diminish chlorophyll abundances. A similar pattern emerged in the North Pacific and Atlantic basins. The model also appeared to overestimate chlorophyll in the Antarctic in austral summer, which may be due to iron limitation.

The other Southern Hemisphere basins (Indian, Pacific, and Atlantic) also exhibited little interannual variability for the SeaWiFS record under investigation here. A prominent recurring seasonal signal was apparent, however, with maxima corresponding to the austral winter, when mixed-layer deepening entrained nutrients into the depleted euphotic zone. The model appeared to represent these dynamics in these basins.

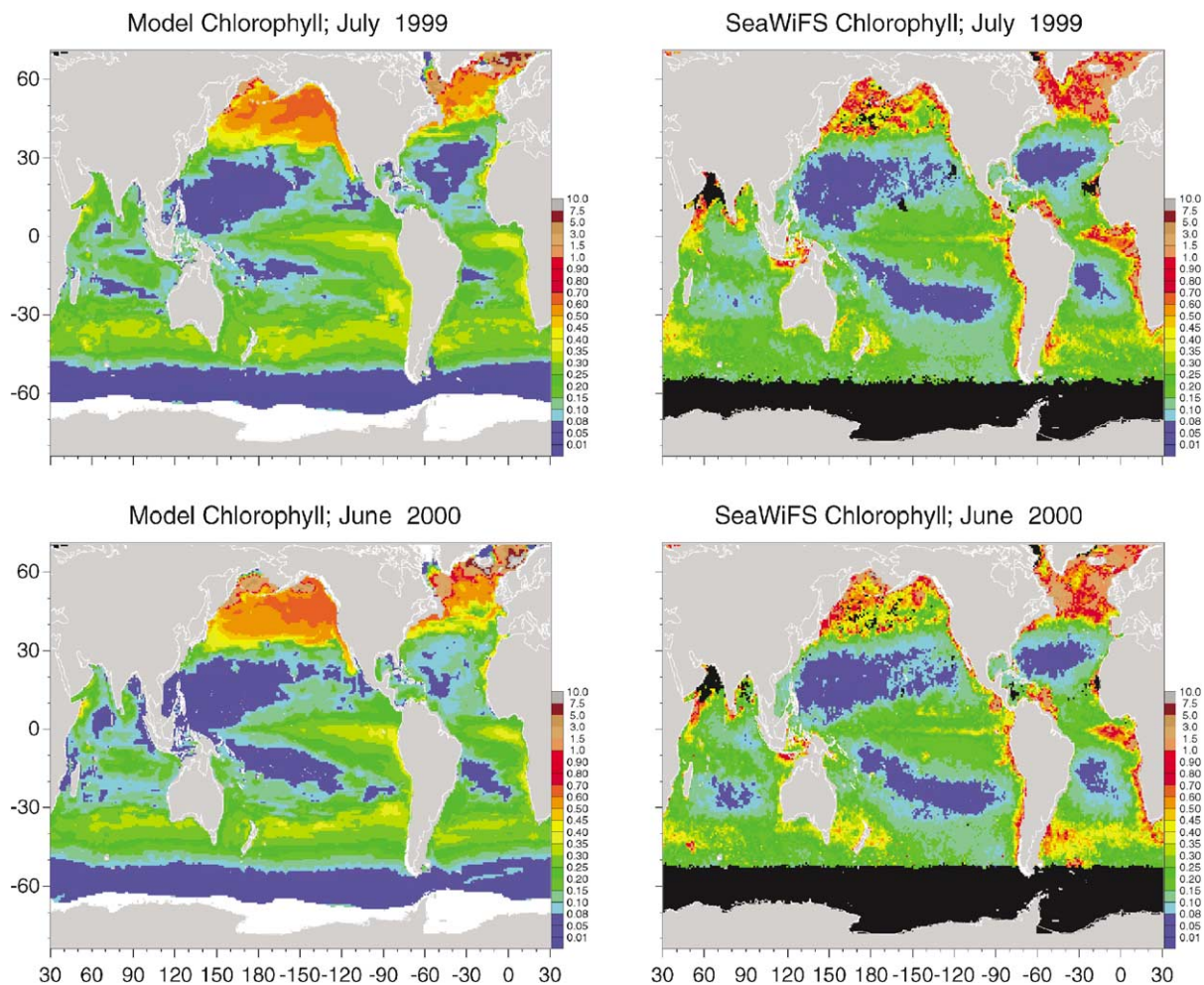


Fig. 12. Top: Mean monthly model chlorophyll for July 1999 compared with SeaWiFS data. Bottom: June 2000. In July 1999 an intense bloom of chlorophyll has developed in the equatorial Atlantic. A similar feature appears in the model but not as intense. Similar patterns of high latitude blooms are observed in the Northern Hemisphere. By June 2000 more normal chlorophyll patterns have arrived, but with possibly continued exceptional upwelling in the equatorial Atlantic.

3.3. Interannual variability in phytoplankton group distributions

Model phytoplankton group distributions exhibited significant departures from climatological conditions in some basins during the nearly 3-year SeaWiFS record. These observations are difficult to confirm with in situ observations, because of how recent the SeaWiFS observations are and how sparse phytoplankton group data can be. Nevertheless, the model results can provide some insight into the mechanisms governing basin-scale phytoplankton group changes, and can provide hypotheses as to the nature of interannual variability.

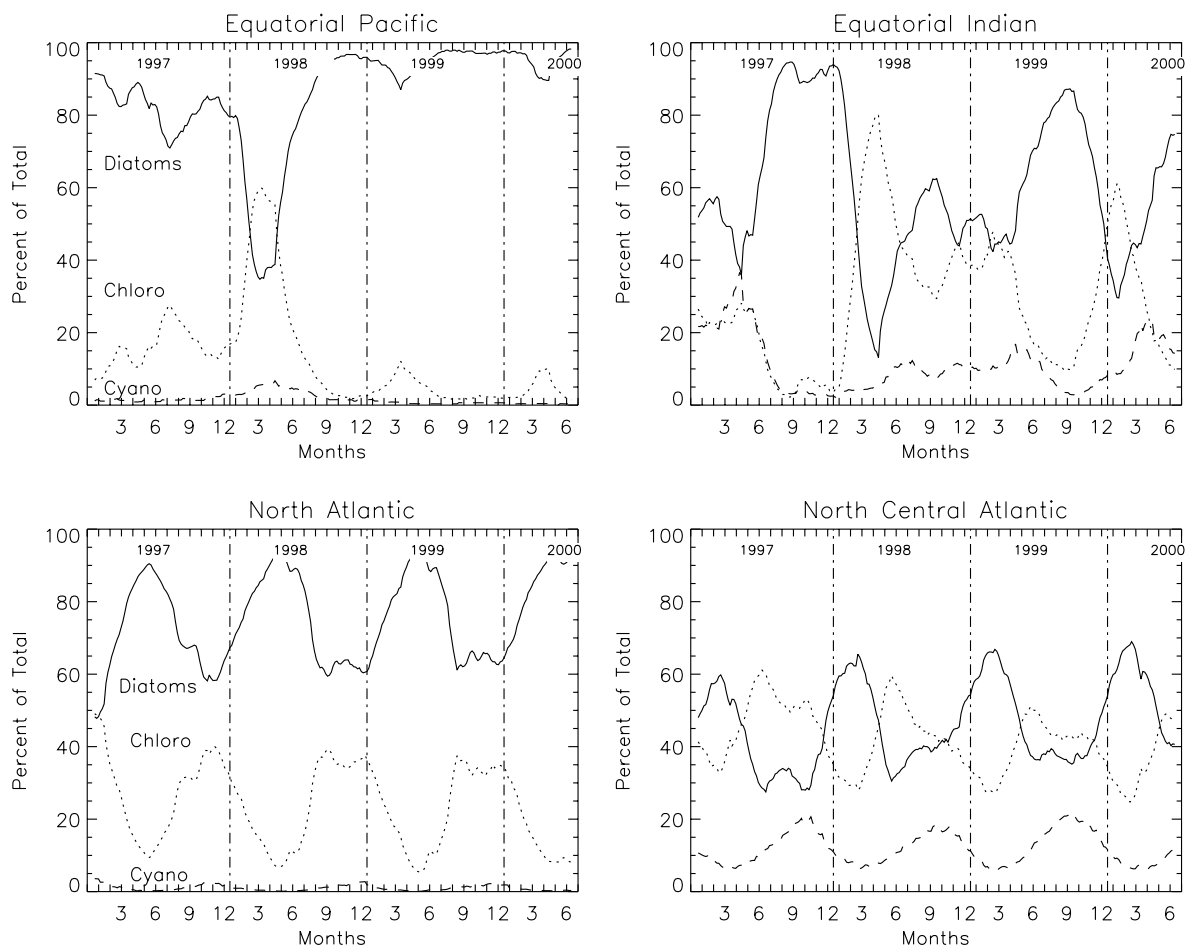


Fig. 13. Phytoplankton group distributions during the SeaWiFS record in 4 basins. Top left: eastern Equatorial Pacific (only the portion east of -100° longitude), where diatoms predominated the La Niña period but not the El Niño. Top right: eastern Equatorial Indian (only the portion east of 90° longitude), where diatoms predominated the El Niño, but other groups predominated in the La Niña. Bottom left: North Atlantic, showing overall diatoms predominance but shifting in winter to cyanobacteria. Bottom right: North Central Pacific, which exhibited little compositional change as a function of interannual variability.

The largest interannual variability in phytoplankton distributions occurred in the equatorial Pacific and Indian Oceans, where the El Niño and La Niña events were most prominent. In the eastern tropical Pacific (-100° to -70° longitude), diatom populations diminished as the El Niño persisted, reaching a minimum at the nominal end of the event in May 1998 (Fig. 13). During this time, diatoms were replaced by chlorophytes, and cyanobacteria increased their relative abundances. With the end of the El Niño and the beginning of the La Niña, diatom relative abundance increased and eventually reached a larger proportion than before the El Niño. These results conform to observations by Chavez et al. (1999), who noted that in the tropical Pacific, El Niño is dominated by pico and nanoplankton, and the La Niña brings about the increased relative

abundance of diatoms. In the model this was caused by nutrient supply. With their relatively rapid sinking rates, the reduced nutrient availability in El Niño was insufficient for diatoms to maintain their populations, and the slower growing but slower sinking chlorophytes and cyanobacteria attained a competitive advantage. Enhanced nutrient supply provided by intensified upwelling of La Niña favored the faster growing diatoms.

A different pattern emerged from the El Niño in the tropical Indian Ocean. Here the main effect of El Niño was to produce intensified upwelling in the eastern portion of the basin (east of 90° longitude; Fig. 13). Although the pattern of phytoplankton group relative abundance was dissimilar from the Pacific, the same biological and physical principles were at work. Thus the increased upwelling in the eastern Indian Ocean during the establishment of El Niño produced greater nutrient supply, and diatom populations increased their abundances relative to the other groups (Fig. 13). As the El Niño progressed into 1998, a shutdown of nutrient supply occurred, resulting in replacement of diatoms by chlorophytes. This replacement occurred in parallel with diminishing chlorophyll (Fig. 8). Re-establishment of more normal circulation patterns arriving with La Niña resulted in increased diatom populations, and the decrease of chlorophytes and cyanobacteria (Fig. 13), although diatom populations did not attain concentrations as large as in the El Niño.

In the North Atlantic, diatoms predominated throughout the SeaWiFS record, with chlorophytes increasing their relative abundance in late boreal summer/fall (Fig. 13). There was very little evidence of interannual variability in the phytoplankton group distributions here.

The North Central Atlantic exhibited subtle interannual variability (Fig. 13). It indicated a pattern of diatom predominance in boreal winter and early spring, yielding to chlorophyte predominance in summer and fall. Cyanobacteria relative abundances increased in the boreal fall and decreased in early spring summer in a pattern that was out of phase with diatoms and chlorophytes. Subtle indications of interannual variability included earlier dominance of diatoms in late 1998–early 1999, slightly larger predominance of diatoms in winter 1999, corresponding to the increased upwelling off Mauritania, and depressed chlorophyte relative abundances in spring/summer 1999 compared to 1997 and 1998.

4. Conclusions

The nearly 3-year SeaWiFS record from launch (September 1997) to June 2000 has given us our first comprehensive glimpse of interannual variability of ocean chlorophyll dynamics. Moreover, SeaWiFS was launched as one of the largest El Niño events was underway, and which eventually gave way to one of the largest, most intensive, and longest-lasting La Niña events ever recorded (continuing at the end of the record). The SeaWiFS chlorophyll record captured the response of ocean phytoplankton to these significant events in the tropical Indo-Pacific basins, but also indicated significant interannual variability unrelated to the El Niño/La Niña. This included large variability in the North Atlantic and Pacific basins, large variability in the North Central and equatorial Atlantic, and milder patterns in the North Central Pacific, the latter of which may be due partially to the El Niño. The Southern Hemisphere exhibited, in contrast, relatively little interannual variability during the SeaWiFS record.

We are fortunate to live in an era when global atmospheric data sets are routinely and nearly immediately available. Thus we have the opportunity to drive a coupled physical/biogeochemical/radiative model of the global oceans with actual near-real-time forcing data such as wind stresses, SSTs, shortwave radiation, and sea ice. Our only limitation is cloud cover and thickness data, which are necessary to evaluate the spectral irradiance with depth, which drives phytoplankton dynamics. Although this is a shortcoming, the availability of the other forcing data gives us an opportunity to track the SeaWiFS record with a global coupled model and attempt to provide physically and biogeochemically meaningful explanations of the variability observed in the SeaWiFS data set.

Even without cloud data, the coupled model was able to represent the seasonal distributions of chlorophyll during the SeaWiFS era, and was capable of differentiating among the widely different processes and dynamics occurring in the global oceans. The model was also reasonably successful in representing the interannual signal, especially when it was large, such as the El Niño and La Niña events in the tropical Pacific and Indian Oceans. In these two regions the model provided different phytoplankton group responses for the different events. The interannual variability in the North Pacific, which was exhibited in SeaWiFS data as an increase in the spring bloom in 1999 and 2000 relative to 1998, was represented and resulted in the model from a more rapidly shoaling mixed layer, inhibiting herbivore population development, thus preventing maximum and immediate utilization of available nutrients from winter convection. However, several aspects of the interannual cycle were not well-represented by the model. Some of which may be due to the model deficiencies of a lack of topographic and coastal influences such as the North Indian Ocean, some may be related to the lack of monthly cloud data, some may be due to riverine influences missing in the model such as the equatorial Atlantic, and finally some may be the result of biases in SeaWiFS atmospheric correction procedures such as absorbing aerosols which are common in the equatorial and mid-latitude eastern Atlantic and the North and equatorial Indian Oceans. Nevertheless, broad agreement suggests confidence in the large scale (synoptic and basin scale) processes in the model and its ability to provide plausible explanations for some the variability observed in this unique spaceborne data set.

Acknowledgements

Development of the OGCM was by Paul Schopf, Climate Dynamics Program, School for Computational Sciences, George Mason University. The NASA/GSFC/DAAC provided the CZCS and SeaWiFS data that was used for comparison. NCEP reanalyses were made available by the Climate Diagnostics Center. Nancy Casey McCabe, Science Systems and Applications, Inc, Larham, MD, obtained the atmospheric forcing data sets, re-gridded when necessary to common format and obtained information on weather events during 1998 and 1999. This work was supported under NASA Grant (RTOP) 971-622-51-31.

References

- Arrigo, K.R., Sullivan, C.W., 1994. A high resolution bio-optical model of microalgal growth: tests using sea-ice algal community time-series data. *Limnology and Oceanography* 39, 609–631.

- Arrigo, K.R., Robinson, D.H., Sullivan, C.W., 1995. Vertical profiles of bio-optical and photophysiological properties of sea ice microalgae within the platelet layer of McMurdo Sound, Antarctica. *Journal of Phycology* 98, 173–185.
- Carpenter, E.J., Romans, K., 1991. Major role of the cyanobacterium *Trichodesmium* in nutrient cycling in the North Atlantic Ocean. *Science* 254, 1356–1358.
- Chavez, F.P., Strutton, P.G., McPhaden, M.J., 1998. Biological-physical coupling in the central Equatorial Pacific during the onset of the 1997–1998 El Niño. *Geophysical Research Letters* 25, 3543–3546.
- Chavez, F.P., Strutton, P.G., Friederich, G.E., Feely, R.A., Feldman, G.C., Foley, D.G., McPhaden, M.J., 1999. Biological and chemical response of the Equatorial Pacific to the 1997–98 El Niño. *Science* 286, 2126–2131.
- Conkright, M.E., Levitus, S., Boyer, T.P., 1994. World ocean atlas, Vol. 1: nutrients. NOAA Atlas NESDIS 1, 150pp.
- Conkright, M.E., O'Brien, T., Levitus, S., Boyer, T.P., Stephens, C., Antonov, J., 1998a. World ocean atlas 1998 Vol. 10. Nutrients and chlorophyll of the Atlantic Ocean. NOAA Atlas NESDIS 36, US Government Printing Office, Washington DC, 217pp.
- Conkright, M.E., O'Brien, T., Levitus, S., Boyer, T.P., Stephens, C., Antonov, J., 1998b. World ocean atlas 1998 Vol. 11. Nutrients and chlorophyll of the Pacific Ocean. NOAA Atlas NESDIS 37, US Government Printing Office, Washington DC, 217pp.
- Conkright, M.E., O'Brien, T., Levitus, S., Boyer, T.P., Stephens, C., Antonov, J., 1998c. World ocean atlas 1998 Vol. 12. Nutrients and chlorophyll of the Indian Ocean. NOAA Atlas NESDIS 38, US Government Printing Office, Washington DC, 217pp.
- Dugdale, R.C., Goering, J.J., 1967. Uptake of new and regenerated forms of nitrogen in primary productivity. *Limnology and Oceanography* 12, 196–206.
- Dutkiewicz, S., Follows, M., Marshall, J., Gregg, W.W., 2001. Interannual variability of phytoplankton abundances in the north atlantic. *Deep-Sea Research II* 48, 2323–2344.
- Eppley, R.W., Peterson, B.J., 1979. Particulate organic matter flux and planktonic new production in the deep ocean. *Nature* 282, 677–680.
- Feldman, G.C., Kuring, N., Ng, C., Esaias, W., McClain, C.R., Elrod, J., Maynard, N., Endres, D., Evans, R., Brown, J., Walsh, S., Carle, M., Podesta, G., 1989. Ocean color: availability of the global set. *Eos Transactions of the AGU* 70, 634–641.
- Gregg, W.W., 2000. A coupled ocean general circulation, biogeochemical, and radiative model of the global oceans: seasonal distributions of ocean chlorophyll and nutrients. NASA Technical Memorandum 2000-209965, 33pp.
- Gregg, W.W., Carder, K.L., 1990. A simple spectral solar irradiance model for cloudless maritime atmospheres. *Limnology and Oceanography* 35, 1657–1675.
- Gregg, W.W., Walsh, J.J., 1992. Simulation of the 1979 spring bloom in the Mid-Atlantic Bight: a coupled physical/biological/optical model. *Journal of Geophysical Research* 97, 5723–5743.
- Le Comte, D., 2000. weather around the world. *Weatherwise* 54, 24–29.
- McClain, M.E., Richey, J.E., Brandes, J.A., Pimentel, T.P., 1997. Dissolved organic matter and terrestrial-lotic linkages in the central Amazon basin of Brazil. *Global Biogeochemical Cycles* 11, 295–312.
- McClain, C.R., Cleave, M.L., Feldman, G.C., Gregg, W.W., Hooker, S.B., Kuring, N., 1998. Science quality SeaWiFS data for global biosphere research. *Sea Technology* September, 10–16.
- McClain, C.R., Ainsworth, E.J., Barnes, R.A., Eplee, R.E., Patt, F.S., Robinson, W.D., Wang, M., Bailey, S.W., 2000a. SeaWiFS postlaunch calibration and validation analyses, part 1. NASA Technical Memorandum-2000-206892, Vol. 9. 82 pp.
- McClain, C.R., Barnes, R.A., Eplee, R.E., Franz, B.A., Hsu, N.C., Patt, F.S., Pietras, C.M., Robinson, W.D., Schieber, B.D., Schmidt, G.M., Wang, M., Bailey, S.W., Werdell, P.J., 2000b. SeaWiFS postlaunch calibration and validation analyses, part 2. NASA Technical Memorandum-2000-206892, Vol. 10. 57 pp.
- McGillicuddy, D.J., Robinson, A.R., McCarthy, J.J., 1995. Coupled physical and biological modelling of the spring bloom in the North Atlantic (II): three dimensional bloom and post-bloom processes. *Deep-Sea Research I* 8, 1359–1398.
- McPhaden, M.J., 1999. Genesis and evolution of the 1997–1998 El Niño. *Science* 283, 950–954.
- McPhaden, M.J., Yu, X., 1999. Equatorial waves and the 1997–1998 El Niño. *Geophysical Research Letters* 26, 2961–2964.

- Monger, B., McClain, C., Murtugudde, R., 1997. Seasonal phytoplankton dynamics in the eastern tropical Atlantic. *Journal of Geophysical Research* 102, 12389–12411.
- Murtugudde, R.G., Signorini, S.R., Christian, J.R., Busalacchi, A.J., McClain, C.R., Picaut, J., 1999. Ocean color variability of the tropical Indo-Pacific basin observed by SeaWiFS during 1997–1998. *Journal of Geophysical Research* 104, 18351–18366.
- O'Reilly, J.E., Maritorena, S., O'Brien, M.C., Siegel, D.A., Toole, D., Menzies, D., Smith, R.C., Mueller, J.L., Mitchell, B.G., Kahru, M., Chavez, F.P., Chavez, P., Strutton, P., Cotta, G.F., Hooker, S.B., McClain, C.R., Carder, K.L., Muller-Karger, F., Harding, L., Magnuson, A., Phinney, D., Moore, G.F., Aiken, J., Arrigo, K.R., Letelier, R., Culver, M., 2000. SeaWiFS postlaunch calibration and validation analyses, part 3. NASA Technical Memorandum-2000-206892, Vol. 11. 49 pp.
- Pacanowski, R.C., Philander, G., 1981. Parameterization of vertical mixing in numerical models of the tropical ocean. *Journal of Physical Oceanography* 11, 1442–1451.
- Reynolds, R.W., Smith, T.M., 1994. Improved global sea surface temperature analyses using optimum interpolation. *Journal of Climate* 7, 75–86.
- Robinson, D.H., Arrigo, K.R., Kolber, Z., Gosselin, M., Sullivan, C.W., 1998. Photophysiological evidence of nutrient limitation of platelet ice algae in McMurdo Sound, Antarctica. *Journal of Phycology* 34, 788–797.
- Sarmiento, J.L., Slater, R.D., Fasham, M.J.R., Ducklow, H.W., Toggweiler, J.R., Evans, G.T., 1993. A seasonal three-dimensional ecosystem model of nitrogen cycling in the North Atlantic euphotic zone. *Global Biogeochemical Cycles* 7, 417–450.
- Schopf, P.S., Loughe, A., 1995. A reduced gravity isopycnal ocean model: Hindcasts of El Nino. *Monthly Weather Review* 123, 2839–2863.
- Shimoda, H., 1999. ADEOS overview. *IEEE Transactions on Geoscience and Remote Sensing* 37, 1465–1471.
- Siegel, D.A., McGillicuddy, D.J., Fields, E.A., 1999. Mesoscale eddies, satellite altimetry, and new production in the Sargasso Sea. *Journal of Geophysical Research* 104, 13359–13379.
- Signorini, S.R., Murtugudde, R.G., McClain, C.R., Christian, J.R., Picaut, J., Busalacchi, A.J., 1999. Biological and physical signatures in the tropical and subtropical Atlantic. *Journal of Geophysical Research* 104, 18367–18382.
- Slingo, A., 1989. A GCM parameterization for the shortwave radiative properties of water clouds. *Journal of Atmospheric Science* 46, 1419–1427.
- Smith, W.O., Nelson, D.M., 1986. Importance of ice-edge phytoplankton production in the Southern Ocean. *BioScience* 36, 251–256.
- Yoder, J.A., McClain, C.R., Feldman, G.C., Esaias, W.E., 1993. Annual cycles of phytoplankton chlorophyll concentrations in the global ocean: a satellite view. *Global Biogeochemical Cycles* 7, 181–193.
- Walsh, J.J., Dieterle, D.A., Muller-Karger, F.E., Bohrer, R., Bissett, W.P., Varela, R.J., Aparicio, R., Diaz, R., Thunell, R., Taylor, G.T., Scranton, M.I., Fanning, K.A., Peltzer, E.T., 1999. Simulation of carbon–nitrogen cycling during spring upwelling in the Cariaco Basin. *Journal of Geophysical Research* 104, 7807–7825.